TIGAR alleviates oxidative stress in brain with extended ischemia via a pentose phosphate pathway-independent manner

Mengru Liu [a,1], Xinyu Zhou [a,1], Yue Li [a], Shijia Ma [a], Ling Pan [a], Xingxian Zhang [a], Wanqing Zheng [a], Zhanxun Wu [a], Ke Wang [a], Anil Ahsan [a], Jiaying Wu [b], Lei Jiang [a], Yangyang Lu [a], Weiwei Hu [a], Zhenghong Qin [c], Zhong Chen [a,d,**], Xiangnan Zhang [a,e,*]

[a] *Institute of Pharmacology & Toxicology, College of Pharmaceutical Sciences, Key Laboratory of Medical Neurobiology of the Ministry of Health of China, Zhejiang University, 310058, Hangzhou, China*
[b] *The First Affiliated Hospital, College of Medicine, Zhejiang University, 310003, Hangzhou, China*
[c] *Department of Pharmacology, Laboratory of Aging and Nervous Diseases, Jiangsu Key Laboratory of Neuropsychiatric Diseases, College of Pharmaceutical Science, Soochow University, Suzhou, 215123, China*
[d] *Key Laboratory of Neuropharmacology and Translational Medicine of Zhejiang Province, College of Pharmaceutical Sciences, Zhejiang Chinese Medical University, Hangzhou, 310053, China*
[e] *Jinhua Institute of Zhejiang University, 321299, Jinhua, China*

ARTICLE INFO

ABSTRACT

TP53-induced glycolysis and apoptosis regulator (TIGAR) alleviates oxidative stress and protects against ischemic neuronal injury by shifting glucose metabolism into the pentose phosphate pathway (PPP). However, the brain alters glucose metabolism from PPP to glycolysis during prolonged ischemia. It is still unknown whether and how TIGAR exerts the antioxidant activity and neuroprotection in prolonged ischemic brains. Here, we determined the significant upregulation of TIGAR that was proportional to the duration of ischemia. However, TIGAR failed to upregulate the NADPH level but still alleviated oxidative stress in neuronal cells with prolonged oxygen glucose-deprivation (OGD). Furthermore, inhibiting PPP activity, either by the expression of mutant TIGAR (which lacks enzymatic activity) or by silencing Glucose 6-phosphate dehydrogenase, still retained antioxidant effects and neuroprotection of TIGAR with prolonged OGD. Intriguingly, TIGAR-induced autophagy alleviated oxidative stress, contributing to neuron survival. Further experiments indicated that TIGAR-induced autophagy neutralized oxidative stress by activating Nrf2, which was cancelled by ML385 or *Nrf2* knockdown. Remarkably, either *Atg7* deletion or *Nrf2* silencing abolished the neuroprotection of TIGAR in mice with prolonged ischemia. Taken together, we found a PPP-independent pathway in which TIGAR alleviates oxidative stress. TIGAR induces autophagy and, thus, activates Nrf2, offering sustainable antioxidant defense in brains with extended ischemia. This previously unexplored mechanism of TIGAR may serve as a critical compensation for antioxidant activity caused by the lack of glucose in ischemic stroke.

1. Introduction

Brains are highly vulnerable to oxidative stress caused by ischemic stroke [1]. The brain has developed a variety of mechanisms to meet the need of antioxidant activity during ischemia. Nicotinamide adenine dinucleotide phosphate (NADPH) serves as the primary reductant to neutralize the oxidants [2]. In neurons, NADPH is mainly generated from glucose metabolism via the pentose phosphate pathway (PPP), which is negatively regulated by fructose-2,6-bisphosphate (Fru-2,6-BP) [3]. The TP53-induced glycolysis and apoptosis regulator (TIGAR) acts as a fructose-2,6-bisphosphatase (Fru-2,6-BPase), which catalyzes Fru-2, 6-BP to fructose-6-phosphate. Therefore, TIGAR directs glucose to the

PPP [4,5]. This metabolic feature allows neurons to cope with oxidative stress. Indeed, TIGAR depletion exhausts NADPH and aggravates ischemic neuronal injury [6]. Conversely, NADPH supplementation alleviates oxidative injury and excitotoxicity caused by cerebral ischemia [7,8]. These studies indicate a crucial role for TIGAR-NADPH in neurons for the defense against ischemia-induced oxidative stress.

An ample supply of glucose is necessary for NADPH generation through PPP. Although cerebral blood flow can be restored after transient ischemia [9], evidence has indicated that most individuals suffering from stroke exist insufficient blood flow in prolonged ischemia [10]. In addition, glucose is predominantly metabolized by glycolysis, rather than the PPP, upon reperfusion [11]. Paradoxically, neuronal TIGAR shows a four-fold upregulation after 2 h of ischemia [6], which can be sustained as long as 24 h after ischemia in mice [12]. It remains largely unexplored whether TIGAR-NADPH may play a role in counteracting oxidation caused by prolonged cerebral ischemia.

Stressed mitochondria and peroxisomes are the primary source of reactive oxygen species (ROS) in ischemic neurons [13,14]. Oxidation serves as a signal to activate autophagy, which neutralizes oxidative stress through autophagic degradation of dysfunctional mitochondria and peroxisomes in neurons [15,16]. Emerging evidence indicates that TIGAR either inhibits [8,17–20] or activates autophagy [21,22] under different conditions. However, it is unclear whether the TIGAR-activated autophagy contributes to antioxidation.

In the present study, we determined to characterize whether and how TIGAR promotes antioxidant activity and neuroprotection with extended ischemia. Unexpectedly, we found that, upon prolonged ischemia, TIGAR attenuated oxidative stress in a PPP-independent manner. Instead, TIGAR induced autophagy and thus activated Nrf2 to maintain the redox balance in prolonged ischemia.

2. Materials and methods

2.1. Animals

Male C57BL/6 mice weighing 22–25 g (8–10 weeks old) were used. Mice were raised on a 12 h/12 h light/dark cycle with *ad libitum* access to water and food. The *Atg7$^{fl/fl}$* mice were kindly provided by Masaaki Komatsu (Tokyo Metropolitan Institute of Medical Science, Tokyo, Japan). All experiments were approved by and conducted in accordance with the ethical guidelines of the Zhejiang University Animal Experimentation Committee and were in complete compliance with the National Institutes of Health Guide for the Care and Use of Laboratory Animals. Efforts were made to reduce any suffering and the number of animals required.

2.2. Middle cerebral artery occlusion (MCAO) in mice

Mice were anesthetized with isoflurane during surgery. Cerebral blood flow (CBF) was monitored in the middle cerebral artery (MCA) by laser Doppler flowmetry (Moor Instruments). A fiber-optic probe was placed over the skull from 2-mm caudal to bregma and 6-mm lateral to midline over the cortex supplied by the proximal portion of the right MCA. Then a 6-0 nylon monofilament suture (tip passivated and coated with 1% poly-L-lysine) was inserted 10 mm into the internal carotid artery to block the origin of the MCA. Animals were used for the study if the CBF reduced lower than 80%. Mice were given different durations (0.5, 1, 2 or 6 h) of MCAO followed by 3 or 24 h of reperfusion. To monitor the CBF directly after different durations of ischemia, images of CBF were determined by Laser Speckle Imaging System (RWD) at 24 h after MCAO.

To measure infarct volumes, mice were anesthetized with a lethal dose of isoflurane and sacrificed at 24 h after MCAO. Slices of coronal brain (2 mm) were stained with 2,3,5- triphenyltetrazolium chloride (TTC; 0.25%; Sigma, T8877) fixed by paraformaldehyde. Brain infarct volumes were determined by an indirect method that corrects for edema

using the Image-Pro Plus software [23].

Neurological deficit scores were evaluated at 24 h after MCAO as follows: 0, no deficit; 1, flexion of contralateral forelimb upon lifting the whole animal by the tail; 2, circling to the contralateral side; 3, falling to the contralateral side; 4, no spontaneous motor activity; and 5, death.

2.3. Delivery of viruses

Mice anesthetized with isoflurane were mounted in a stereotaxic apparatus (Stoelting, 512, 600). To overexpress TIGAR, adeno-associated virus (AAV), including AAV-GFP-vector-3×Flag and AAV-GFP-TIGAR-3×Flag, was injected into the cortex (AP + 0.2 mm; L − 3.2 mm; V − 1.5 mm), (AP + 0.5 mm; L − 0.1 mm; V − 0.05 mm) and corpus striatum (AP + 0.5 mm; L − 2.0 mm; V − 3.0 mm) with a 5 μL syringe (Gaoge Industrial and Trading Co. Ltd, Shanghai, China) controlled by an injection pump (Micro 4, WPI, Sarasota, Fl, USA) at 80 nL/min. The needle was retained for an additional 10 min to prevent backflow of the virus and was then slowly withdrawn. The virus was allowed to express target proteins for a minimum of three weeks. For ablation autophagy in neurons, *Atg7$^{fl/fl}$* mice were injected with AAV-hSyn-Cre-mCherry into the cortex and corpus striatum. To determine the antioxidant capacity and neuroprotection of Nrf2, mice were injected with AAV-mCherry-3×Flag-Nrf2-shRNA into the cortex and corpus striatum. AAV-hSyn-Cre-mCherry was purchased from Shanghai Taitool Bioscience Co. Ltd, Shanghai, China). All other viruses were purchased from OBiO Technolog Co. Ltd, Shanghai, China).

2.4. Cell culture, OGD-Rep, and drug administration

Pregnant mice with embryonic (E17) fetuses were used for primary neuron culture. The experiments were performed as described previously [24]. Briefly, cortical neurons were isolated from fetal mice and digested with 0.25% trypsin (Invitrogen, 25200-056). Then approximately 10^5 cells/cm^2 were seeded onto the poly-L-lysine (Sigma, P1399)–coated microscope coverslips (Fisher Scientific, 12-545-80) for immunostaining; six-well plates for immunoblotting and glass-bottom dishes (Cellvis, D35-20-0-N) were used for live cell confocal imaging. The cortical neurons were cultured in Neurobasal medium (Invitrogen, 21103–049) supplemented with 2% B27 (Invitrogen, 17504–044), 10 U/mL penicillin-streptomycin (Solarbio, P1400) and 0.5 mmol/L glutamine (Gibco, 25030081), at 37 °C in a humidified atmosphere with 5% CO_2. Cultures were maintained for 8d before further treatment and were routinely observed under a phase-contrast inverted microscope.

For SH-SY5Y (human neuroblastoma) cell cultures, cells were grown in Dulbecco's modified Eagle's medium (DMEM, Gibco, 12800-017), supplemented with 10% fetal bovine serum (Biological Industries, 04-001-1ACS) and10 U/ml penicillin-streptomycin (Gibco, 15140–122) at 37°C in a humidified atmosphere with 5% CO_2.

For OGD treatment, the cells were then rinsed with glucose-free DMEM (Invitrogen, 12800–017) to remove residual glucose and refreshed with oxygen- and glucose-free DMEM (pre-balanced in an oxygen free chamber at 37 °C). Cells were then immediately placed in a sealed chamber (Billups Rothenburg, MIC-101) loaded with a gas mixture of 5% CO_2 and 95% N_2 for 7 min. The chambers were sealed and incubated for varying durations of OGD at 37 °C. For neurons, the different durations of OGD were 0.5 and 3 h; for SH-SY5Y, the different durations of OGD were 1, 4 and 6 h. For reperfusion (Rep), cells were refreshed with normal culture medium for 3, 6 or 24 h at 37 °C. Prior to OGD treatment, cells were incubated with the inhibitor, chloroquine (50 μM, Sigma, C6628), for 4 h. 100 nM wortmannin (MedChemExpress, HY-10197) or 3 μM ML385 (Selleck, S8790) was added during OGD-Rep.

2.5. Plasmid transfection and RNA silencing

Primary cultured neurons were transfected with AAVs containing AAV-GFP-vector-3×Flag, AAV-GFP-TIGAR-3×Flag, AAV-mCherry-

3×Flag-shRNA and AAV- mCherry-3×Flag-Nrf2-shRNA. AAVs were incubated with neurons at 6 d *in vitro*.

TIGAR and TIGAR Mutant (H11A/E102A/H198A) were ligated into the 3×Flag-CMV-7.1 vector (Sigma, E7533), pGFP-C1 and pmCherry-C1. The plasmids were then transfected into SH-SY5Y cells according to the jetPRIME (n114–15, Polyplus, France) protocol.

Small interfering RNA (siRNA) targeting human TIGAR (siTIGAR sequences: #1, GAUGAACCUCUUUCAGAAA; #2, GCAAAGAUAU-GACGGUAAA; #3, CCUACAGGAUCAUCUAAAU) [18] and G6PD (siG6PD sequences: #1, UGAUGAAGAGAGUGGGUUU; #2, ACA-GAUACAAGAACGUGAA; #3, AGUCGGAUACACACAUAUU), as well as scramble siRNA (GGACCACCGCAUCUCUACA), were synthesized. After 5 h of transfection, cells were refreshed with DMEM containing 5% fetal bovine serum. After 24 h transfection, the knockdown efficiency of siRNA was determined by immunoblotting.

2.6. Immunoblotting

Brain tissues and cells were homogenized using RIPA buffer. For cytosolic and nuclear protein extraction, Nuclear and Cytoplasmic Extraction Reagents (Thermo Scientific, 78833) was used according to the manufacturer's instructions. A 40-μg aliquot of protein from each sample was separated by SDS-PAGE. The following primary antibodies were used: TIGAR (1:1000; ABclonal, A20416), G6PD (1:1000; ABclonal, A1537), ACTB (1:5000; ABclonal, AC026), Flag (1:1000; Cell Signaling Technology, 14793s), LC3B (1:1000; Sigma-Aldrich, L7543), p62 (1:1000; MBL, PM045), Beclin-1 (1:1000; Cell Signaling Technology, 3495), Atg5 (1:1000; Cell Signaling Technology, 12994), Atg12 (1:1000; Cell Signaling Technology, 4180), TOMM20 (1:1000; ABclonal, A19403), PEX14 (1:1000; ABclonal, A7336), Nrf2 (1:1000; ABclonal, A1244), Histone 3 (1:1000; ABclonal, A2348) and KEAP1 (1:1000; Cell Signaling Technology, 4678). Secondary antibodies conjugated with HRP against either rabbit or mouse IgG (1:3000; Cell Signaling Technology, 7071 and 7072) were applied. Digital images were quantified by densitometric measurement with the Image-Pro Plus software.

2.7. Assessment of ROS

For the assessment of ROS in ischemic brain tissues and neurons, malondialdehyde (MDA) production was measured. At 3 h of reperfusion, brain tissues or medium of neurons were collected and the MDA level was measured using the Micro-MDA Assay Reagent Kit (KeyGEN BioTECH, KGT003-1) according to the manufacturer's protocol. The results were expressed as the fold-change in the MDA level relative to the control in neurons. In addition, the ROS level was also assessed by dihydroethidium (DHE, Sigma, D7008) staining in neurons. Briefly, the neurons were incubated with 2 μM DHE for 30 min at 37 °C in the dark. The cells were then refreshed with PBS and the DHE fluorescence intensity was observed with a confocal microscope (Leica TSC SP8).

For SH-SY5Y cells, intracellular ROS level was measured with a probe 2′,7′- Dichlorodihydrofluorescein diacetate (H2DCFDA, MedChemExpress, HY-D0940). In brief, cells were incubation with 10 μM H2DCFDA for 30 min at 37 °C in the dark. Then cells were harvested with 0.25% Trypsin-EDTA solution, resuspended in phosphate buffer saline (PBS) and immediately analyzed with flow cytometer (Beckman Coulter, Cytoflex) with 488 nm excitation and 521 nm emission for the measurement of fluorescent intensity. The results were expressed as the fold change of mean fluorescence intensity relative to the control cells.

2.8. Measurement of NADPH level

Brain tissues and cells were collected at 3 h of reperfusion. NADPH level were then measured with the EnzyChrom NADP/NADPH assay kit (BioAssay Systems, ECNP007) following the manufacturer's protocol.

2.9. Cell viability assay

For cell viability determination, lactate dehydrogenase (LDH) release from cells was measured. A 120 μL aliquot of medium was removed and the amount of LDH leakage from the cells was determined using the LDH kit (Beyotime, C0017) at 24 h after OGD, according to the manufacturer's protocol. The absorbance of samples was measured using a spectrophotometer at 490 nm. The results were expressed as the fold-change of LDH leakage relative to the control cells.

2.10. Immunostaining and confocal imaging

For immunostaining, cells seeded on the coverslip were fixed in 4% paraformaldehyde for 15 min and washed three times with PBS. The cells were then permeabilized with 0.3% (v/v) Triton X-100 and blocked with 5% (v/v) donkey serum for 2 h. This was followed by incubation with the primary antibodies PEX14 (1:100; ABclonal, A7336) or Nrf2 (1:100; ABclonal, A11159) overnight at 4 °C. Secondary antibodies labeled with Alex Fluor 488 or 647 (Invitrogen, A32731 and A32733) were subsequently added to the cells for 2 h, which were further incubated with DAPI (YEASEN, 36308). The coverslips were observed with a confocal microscope. Five randomly selected fields from one coverslip were included to calculate an average and experiments were repeated independently in at least triplicate.

2.11. Real-time PCR

Neurons were collected with 0.25% trypsin-EDTA solution after 3 h of OGD followed by 24 h of reperfusion. Then RNA was extracted and purified using UNIQ-10 Column Total RNA Purification Kit (Sangon Biotech, 511361) following the manufacturer's protocol. Next, RNA was converted to first-strand cDNA using the PrimeScript™ RT reagent Kit (Takara, RR047A). Aliquots of 3–10 ng of total DNA were analyzed via real-time PCR (RT-PCR) to evaluate the expression of Nrf2 target genes, *HO-1* and *GCLC*. *ACTB* was a house-keeping gene. The primer sequences used were: mouse *HO-1* (Fw: 5′-CGACAGCATGTCCCAGGATT-3'; Rv: 5′-CTGGGTTCTGCTTGTTTCGC-3′), mouse *GCLC* (Fw: 5′-CCTCCTCCT CCAAACTCAGATA-3'; Rv:5′-CCACAAATACCACATAGGCAGA-3′), mouse *ACTB* (Fw:5′-AAATCGTGCGTGACATCAAAGA-3'; Rv:5′-GGC CATCTCCTGCTCGAA-3′). The 2$^{-\Delta\Delta Ct}$ method was used to determine the fold change in relation to mRNA expression.

2.12. Statistical analysis

All data were collected and analyzed in a blind manner. Data are presented as mean ± SEM. Comparations between three or more groups were performed by one-way ANOVA with Turkey's multiple-comparisons test. A *p*-value < 0.05 was considered statistically significant.

3. Results

3.1. TIGAR alleviates oxidative stress independent of PPP in prolonged cerebral ischemia

We determined the expression of TIGAR in response to duration of ischemia. The experiment design was described in Fig. 1A. The mice were subjected to specific duration (0.5, 1 or 2 h) of ischemia by MCAO. The CBF of mice continuously decreased along with ischemia duration (Supplementary Fig. 1A). The expression of TIGAR in ischemic brain tissue was upregulated in correlation with an increase in ischemia duration. After 2 h of MCAO, TIGAR reached approximately 2.29-fold (*p* < 0.05) of that in sham mice. These results were in line with previous findings that TIGAR undergoes significant upregulation after cerebral ischemia [6,12]. Notably, NADPH, the product from glucose metabolism via the PPP, declined as the ischemia duration increased, suggesting

TIGAR failed to further activate PPP to meet the demand under sustained ischemic condition (Fig. 1B–D). The reduction of PPP activity cannot be attributed to the downregulation of Glucose 6-phosphate dehydrogenase (G6PD), a rate-limiting enzyme for PPP activity

(Fig. 1B and C). We next confirmed the incompetence of TIGAR to activate the PPP after prolonged ischemia. Our results showed that TIGAR overexpression significantly reversed the NADPH deficiency in mice brains that experienced 0.5 or 1 h of MCAO. However, TIGAR
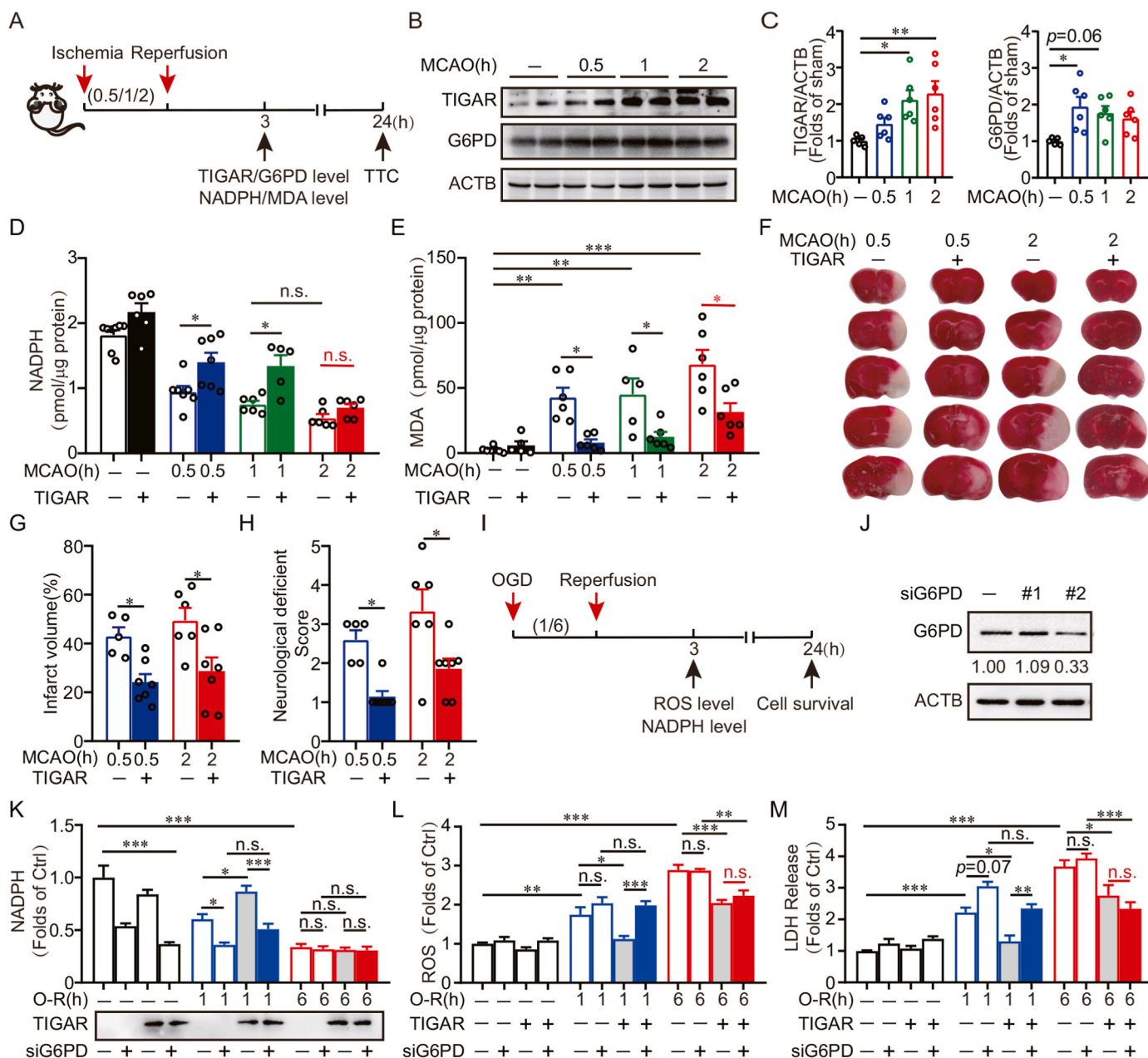
Fig. 1. TIGAR alleviates oxidative stress independent of PPP in prolonged cerebral ischemia. (A) Schematic of surgery protocol for cerebral ischemia in mice. Wild type mice were subjected to different durations (0.5, 1 or 2 h) of occlusion followed by 3 h or 24 h of reperfusion. Experiments were conducted at indicated time of reperfusion. (B) Protein abundance of TIGAR and G6PD were determined by western blot at 3 h of reperfusion. Duplicate lanes are shown for each group. (C) Semi-quantitative analyses of TIGAR and G6PD are shown ($n = 5$–6 mice for each group). (D–H) Wild type mice brains were infected with AAVs expressing GFP -vector-3×Flag, GFP-TIGAR-3×Flag for at least 3 weeks and then subjected to different durations (0.5, 1 or 2 h) of MCAO. (D) NADPH level and (E) MDA level in brain tissues were detected at 3 h of reperfusion. (F) The representative brain slices after TTC staining from each group are shown. (G) Infarct volumes and (H) neurological deficit scores were measured at 24 h of reperfusion ($n = 5$–8 mice for each group). (I) The schematic protocols of oxygen and glucose deprivation (OGD) in SH-SY5Y cells. Cells were subjected to 1 or 6 h of OGD followed by 3 or 24 h of reperfusion. Experiments were conducted at indicated time of reperfusion. (J) Plasmids of G6PD knockdown (siG6PD) were pre-transfected to SH-SY5Y cells and the G6PD level was measured by western blot. Numbers show the semi-quantitative analyses of G6PD. #2 siG6PD plasmid was used for further experiments. (K) SH-SY5Y cells were co-transfected with siG6PD and 3×Flag, 3×Flag-TIGAR and then subjected with 1 or 6 h of OGD. The expression of Flag and NADPH level determined at 3 h of reperfusion. (L and M) SH-SY5Y cells were co-transfected with siG6PD and mCherry-C1, mCherry-TIGAR, mCherry-TIGAR Mutant for 24 h and then subjected with 1 or 6 h of OGD. (L) ROS level was analyzed with H$_2$DCFDA at 3 h of reperfusion. (M) LDH release was measured at 24 h of reperfusion. All experiments are from at least three independent experiments. Data are expressed as mean ± SEM. Statistical comparisons were performed as one-way ANOVA with Turkey's multiple-comparisons test. *$p < 0.05$, **$p < 0.01$, ***$p < 0.001$ versus the indicated group. Ctrl, control.

overexpression failed to reverse the NADPH decline in mice subjected to 2 h or 6 h of MCAO (Fig. 1D, Supplementary Fig. 2A). These data supported the notion that PPP activity was impaired with prolonged cerebral ischemia [11].

We next asked whether TIGAR can offer antioxidant activity to brains with prolonged ischemia. As a control, TIGAR overexpression alleviated the oxidative stress in brains with 0.5 or 1 h MCAO, as reflected by reduced malondialdehyde (MDA) level. Unexpectedly, reinforced TIGAR expression was still competent to reduce MDA in the brain with 2 h or 6 h of MCAO (Fig. 1E, Supplementary Fig. 2B), regardless unreversed level of NADPH (Fig. 1D). As a result, TIGAR overexpression attenuated infarct volumes and neurological deficit in mice that experienced 2 h of MCAO (Fig. 1F–H). Collectively, these results indicated that TIGAR alleviates oxidative injury in prolonged ischemia possibly via a PPP-independent mechanism.

We further identified the PPP-independent antioxidant activity of TIGAR in cultured SH-SY5Y cells. To this end, we transfected the cells with mutant TIGAR (H11A/E102A/H198A), which failed to promote glucose metabolism via the PPP [4]. The SH-SY5Y being subjected to OGD. Exogenous TIGAR, but not mutant TIGAR, reversed the NADPH decline in cells that experienced 0.5 h or 1 h of OGD. In contrast, both TIGAR genotypes failed to rescue NADPH loss in cells with 6 h of OGD (Supplementary Fig. 3A), recapitulating the PPP insufficiency observed in ischemic mice brain. However, we found both the wild-type and mutant TIGAR significantly reversed ROS burst in cells subjected to 6 h of OGD (Supplementary Fig. 3B). Consequently, both genotypes of TIGAR overexpression ameliorated OGD-caused cell death (Supplementary Fig. 3C). These results indicated that Fru-2,6-BPase activity was not required for TIGAR to neutralize oxidative stress after prolonged ischemia. To verify this notion, we knocked down G6PD in SH-SY5Y cells (Fig. 1J) that overexpressed TIGAR. Silencing of G6PD abolished NADPH production by TIGAR in cells with 1 h, but not 6 h, of OGD (Fig. 1K). Furthermore, compared with the results after 1 h of OGD, G6PD silencing failed to abolish the antioxidation and the neuroprotection of TIGAR in cells with 6 h of OGD (Fig. 1L and M). Collectively, these data confirmed the contribution of TIGAR-NADPH to the antioxidant activity in brains with transient ischemia. Remarkably, we identified a PPP-independent antioxidant activity of TIGAR in prolonged cerebral ischemia.

3.2. TIGAR induces autophagy in cells with prolonged OGD

Autophagy alleviated oxidative stress by eliminating damaged organelles that generate ROS in ischemic brains [15,16]. TIGAR inhibits autophagy by directing glucose metabolism into the PPP [8,17–20]. However, emerging studies have indicated an autophagy-activating role of TIGAR under stress conditions [21,22]. We thus hypothesized that TIGAR reduces oxidative stress via the autophagic clearance of mitochondria and peroxisomes after prolonged ischemia. To this end, the expression of LC3B-II and p62 [25], which reflect autophagy flux, were examined by immunoblot in cultured SH-SY5Y cells. It showed LC3B-II decreased and p62 increased with TIGAR overexpression after 1 h of OGD, indicating autophagy inhibition [8,17–20]. On the contrary, TIGAR increased LC3B-II and decreased p62 expression after 6 h of OGD, suggesting autophagy activation (Fig. 2A and B). Additionally, LC3B-II and p62 were further accumulated by the lysosome inhibitor, chloroquine (CQ), indicating autophagy activation rather than lysosome dysfunction (Fig. 2C). Conversely, in cells with TIGAR silencing, the numbers of LC3 puncta increased with 1 h of OGD but decreased with 6 h of OGD (Supplementary Fig. 2 and 2D). In addition, the expression of LC3B-II was decreased and p62 was increased in cells with 6 h, but not 1 h, of OGD (Fig. 2E). These data indicated the discrepant roles of TIGAR in regulating autophagy along with the duration of OGD. Particularly, TIGAR activated autophagy in neuronal cells with prolonged OGD.

We further investigated whether TIGAR-induced autophagy dependents on PPP. As a control, ectopic TIGAR expression suppressed autophagy activation by 1 h of OGD. However, the overexpression of either TIGAR or mutant TIGAR further activated autophagy in cells with 6 h of OGD, as reflected by increased LC3B-II expression and LC3 puncta and decreased p62 expression (Fig. 2F–H). These data clearly indicated that PPP activity is not required for TIGAR-induced autophagy with prolonged ischemic injury. In line with these findings, we further found that cells that underwent 6 h of OGD had increased Beclin-1 and decreased Atg5 expression, proteins involved in autophagosome biogenesis, as a result of TIGAR (Fig. 2I and J). These data were opposite to previous studies that reported the reduction of Beclin-1 expression as a result of TIGAR in neuronal cells with transient ischemia [20].

3.3. Autophagy is required for the antioxidant activity and neuroprotection of TIGAR

We further confirmed the incompetence of TIGAR to activate the PPP after prolonged ischemia in neurons. Our results showed that TIGAR overexpression significantly reversed the NADPH deficiency in neurons with 0.5, 1 or 2 h, but not 3 h, of OGD (Fig. 3A). However, TIGAR overexpression alleviated oxidative stress in 3 h of OGD-treated neurons (Fig. 3 B). We further verified the autophagy activation effects of TIGAR in primary cultured neurons. Consistent with our observations in SH-SY5Y cells, we found TIGAR increased LC3B-II and decreased p62 expression in neurons that experienced 3 h, but not 0.5 h, of OGD (Fig. 3C). We next clarified whether TIGAR-induced autophagy is essential for its antioxidation after prolonged ischemia. Administration of either wortmannin or CQ (autophagy inhibitors) abolished the TIGAR-conferred antioxidant activity in OGD-treated neurons, as revealed by reversed DHE fluorescence [26] (Fig. 3D and E). Moreover, the neuroprotection of TIGAR was also abolished by wortmannin or CQ, as shown by reversed LDH release (Fig. 3F and G). Collectively, these data indicated that autophagy is required for the antioxidant activity and neuroprotection of TIGAR after prolonged ischemia.

3.4. TIGAR did not induce mitophagy and pexophagy in OGD-treated neuronal cells

Autophagy neutralizes oxidative stress by the selective removal of mitochondria and peroxisomes, termed mitophagy and pexophagy, respectively, in ischemic neuronal cells [15]. We thus assumed TIGAR induces mitophagy and/or pexophagy after prolonged ischemia. We visualized the mitochondria by transfecting the cells with Mito-GFP [27]. We unexpectedly found that TIGAR overexpression did not reduce the area of mitochondria in cells subjected to either 1 or 6 h of OGD (Fig. 4A and B). Peroxisomes were counted by immunostaining of PEX14, a peroxisomal marker. It showed that TIGAR failed to reduce the number of peroxisomes, suggesting intact pexophagy (Fig. 4C and D). In line with the imaging analysis, TIGAR overexpression did not reduce the protein levels of TOMM20 and PEX14, the constitutively expressed markers for mitochondria and peroxisomes, respectively (Fig. 4E). These data indicated that mitophagy and pexophagy did not underlie the antioxidative activity of TIGAR-induced autophagy.

3.5. TIGAR alleviates oxidative stress by activating Nrf2 in ischemic neurons

Nuclear factor erythroid 2-related factor 2 (Nrf2) serves as a master regulator in neuronal antioxidation [28–30]. In ischemic neurons, Nrf2 transcriptionally activates the expression of antioxidant enzymes. Previous studies indicated that neuronal autophagy is involved in the regulation of Nrf2 [31]. Nrf2 binds with the Kelch-like ECH-Associating Protein 1 (KEAP1), which can be degraded by autophagy and the Nrf2 can thus be released and translocated to the nucleus where it transcribes target genes under stress conditions [32,33]. We found that TIGAR overexpression can reduce KEAP1 in OGD-treated primary culture neurons (Fig. 5A). This reduction can be reversed by CQ, suggesting
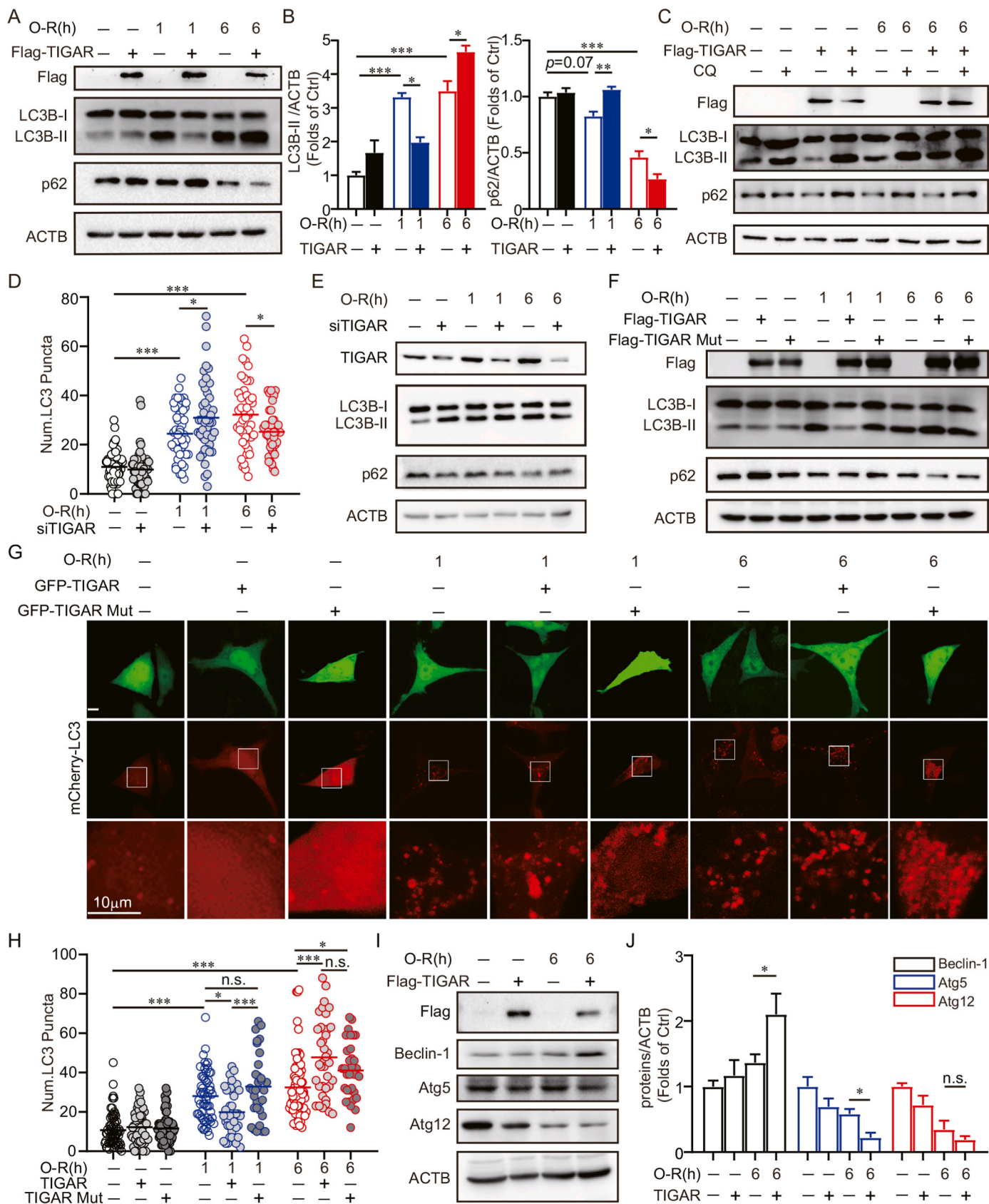
(caption on next page)

Fig. 2. TIGAR induces autophagy in cells with prolonged OGD. (A–C) SH-SY5Y cells were transfected with 3×Flag, 3×Flag-TIGAR for 24 h. (A) SH-SY5Y cells were subjected to 1 or 6 h of OGD followed by 3 h of reperfusion. The Flag, LC3B and p62 levels were determined by western blot. (B) Semi-quantitative analyses of LC3B-II and p62 are shown. (C) SH-SY5Y cells were pretreated with PBS as a vehicle control or 50 μM chloroquine (CQ) for 4 h and then subjected to 6 h of OGD followed by 3 h of reperfusion, the Flag, LC3B and p62 levels were detected by western blot. (D) SH-SY5Y cells were previously co-transfected with mCherry-LC3 and siRNA or siTIGAR and then subjected to 1 or 6 h of OGD followed by 3 h of reperfusion. Columns represent the number of mCherry-LC3–positive puncta ($n = 40$–60 cell for each group). (E) SH-SY5Y cells were previously transfected with siRNA or siTIGAR and then subjected to 1 or 6 h of OGD followed by 3 h of reperfusion. The levels of TIGAR, LC3B, p62 were determined by western blot. (F) SH-SY5Y cells were transfected with 3×Flag, 3×Flag-TIGAR, or 3×Flag-TIGAR-Mutant (H11A/E102A/ H198A) and then subjected to 1 or 6 h of OGD followed by 3 h of reperfusion. The expression of Flag, LC3B and p62 were determined by western blot. (G and H) SH-SY5Y cells were previously co-transfected with mCherry-LC3 and GFP, GFP-TIGAR or GFP-TIGAR-Mutant (H11A/E102A/H198A), then subjected to 1 or 6 h of OGD followed by 3 h of reperfusion. (G) Images shows representative examples of each group from three independent experiments. (H) Columns represent the number of mCherry-LC3–positive puncta ($n = 30$–80 cells for each group). (I and J) SH-SY5Y cells were pre-transfected with 3×Flag or 3×Flag-TIGAR and then subjected with 6 h of OGD followed by 3 h of reperfusion. (I) The levels of Beclin-1, Atg5 and Atg12 were determined by western blot. (J) Semi-quantitative analyses of Beclin-1, Atg5 and Atg12 are shown. All experiments are from at least three independent experiments. Data are expressed as mean ± SEM. Statistical comparisons were performed as one-way ANOVA with Turkey's multiple-comparisons test. *$p < 0.05$, **$p < 0.01$, ***$p < 0.001$ versus the indicated group. Ctrl, control; Num., number.
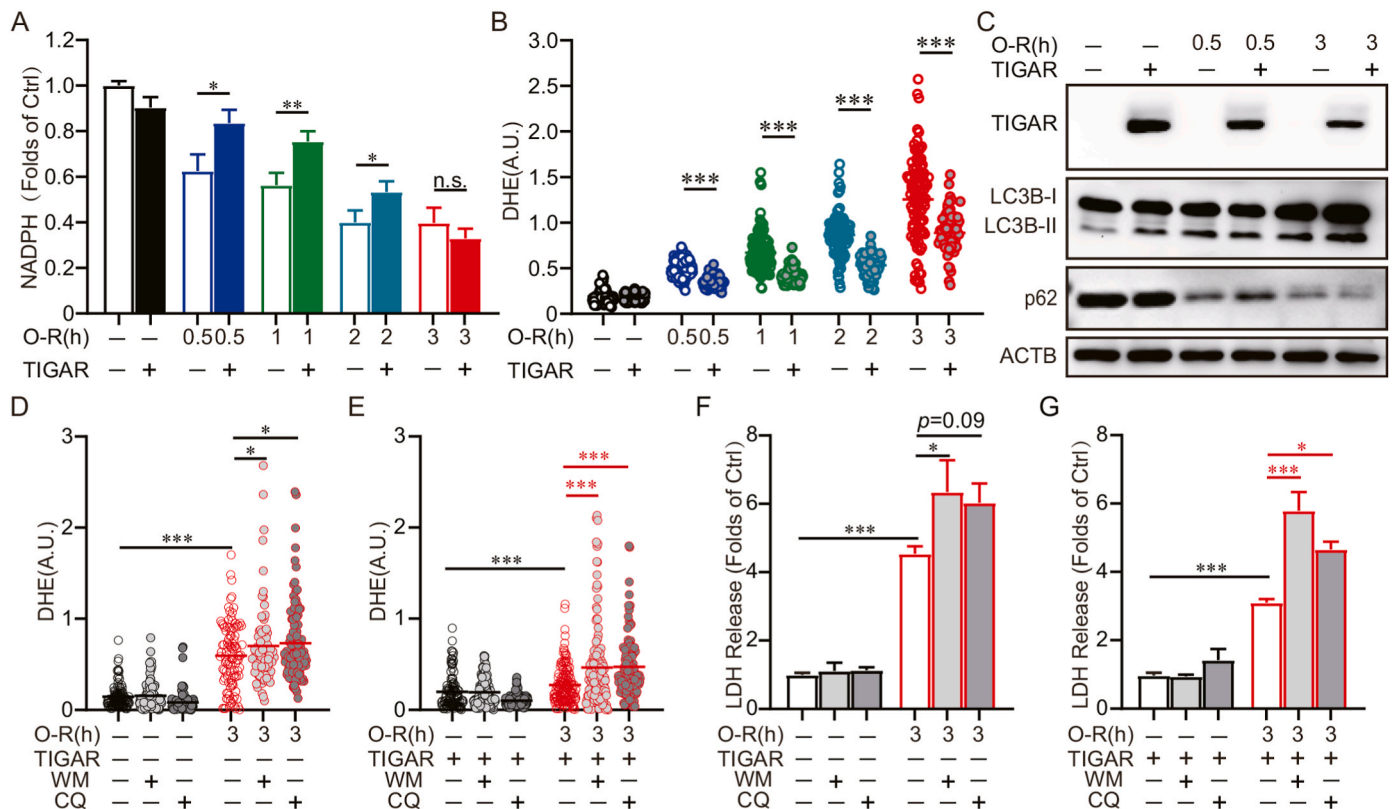
Fig. 3. Autophagy is required for the antioxidant activity and neuroprotection of TIGAR. Primary cultured cortical neurons were transfected with AAVs expressing GFP-vector-3×Flag or GFP-TIGAR-3×Flag at 6 d and then subjected to 0.5, 1, 2 or 3 h of OGD followed by 3 or 24 h of reperfusion at 8 d. (A) NADPH level and (B) DHE fluorescence were detected at 3 h of reperfusion. (C) The Flag, LC3B and p62 levels were determined by western blot at 3 h of reperfusion. (D–G) Primary cultured cortical neurons were pretreated with 50 μM chloroquine (CQ) for 4 h before OGD or 100 nM wortmannin (WM) during OGD-Rep. (D and E) DHE fluorescence revealed ROS level at 3 h of reperfusion ($n = 90$–140 cells for each group). (F and G) LDH release was measured at 24 h of reperfusion. All experiments are from at least three independent experiments. Data are expressed as mean ± SEM. Statistical comparisons were performed as one-way ANOVA with Turkey's multiple-comparisons test. *$p < 0.05$, **$p < 0.01$, ***$p < 0.001$ versus the indicated group. Ctrl, control; A.U., arbitrary units.

autophagic degradation of KEAP1 in ischemic neurons (Fig. 5B). We then determined the subcellular localization of Nrf2 with prolonged OGD. It showed increased Nrf2 abundance in the nucleus as the duration of OGD increased, and can be further enhanced by TIGAR over-expression (Fig. 5C and D). Furthermore, we isolated the nucleus protein fraction from SH-SY5Y cells. The immunoblot results showed that the level of Nrf2 was upregulated in the nucleus after 6 h of OGD, which was further increased with TIGAR transfection. These data confirmed that TIGAR promoted Nrf2 activation with prolonged OGD (Fig. 5E). We further determined whether TIGAR alleviated oxidative stress by the activation of Nrf2 after prolonged ischemia. ML385, an Nrf2 inhibitor [34], abolished the effects of TIGAR on alleviating MDA level and LDH release in OGD-treated cells (Fig. 5F and G). Likewise, Nrf2 silencing

cancelled the antioxidant effect and neuroprotection of TIGAR (Fig. 5H and I). Taken together, these data indicated that TIGAR activated Nrf2, alleviating oxidative stress and preventing neuronal death caused by prolonged ischemia.

3.6. Autophagy is required for TIGAR to activate Nrf2

We next determined the involvement of TIGAR-induced autophagy in Nrf2 activation. These results showed that both TIGAR genotypes induced autophagy in 3 h of OGD-treated neurons (Fig. 6A and B). Furthermore, the TIGAR or mutant TIGAR-facilitated translocation of Nrf2 to the nucleus was reversed by wortmannin in OGD-treated neurons (Fig. 6C and D). It suggested that autophagy was required for
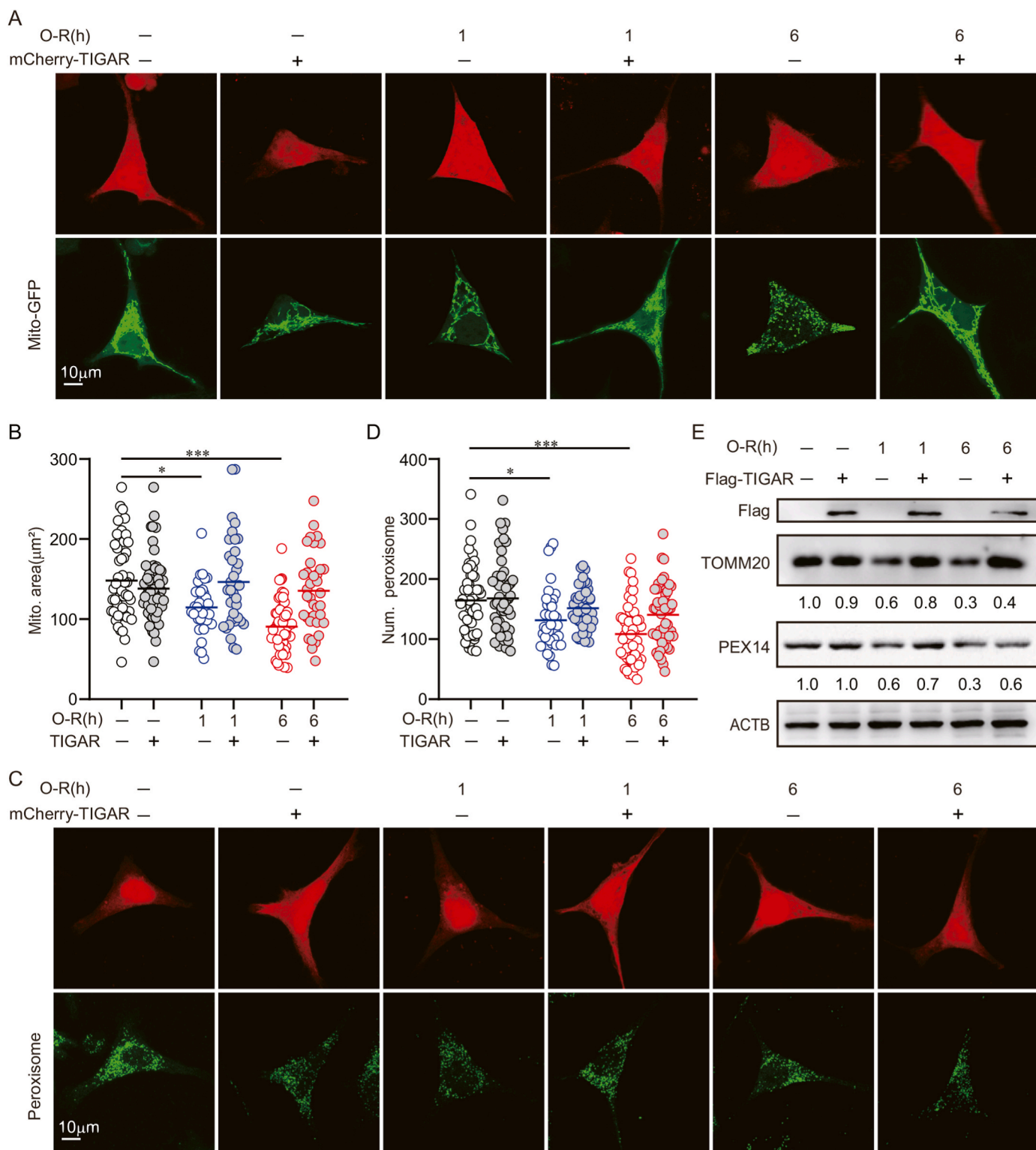
Fig. 4. TIGAR did not induce mitophagy and pexophagy in OGD-treated neuronal cells. (A and B) SH-SY5Y cells were previously co-transfected with Mito-GFP and mCherry-C1 or mCherry-TIGAR and then subjected to 1 or 6 h of OGD followed by 6 h of reperfusion. (A) Images shows representative examples from three independent experiments. (B) Columns represent the area of mitochondria ($n = 30$–60 cells for each group). (C and D) SH-SY5Y cells were pre-transfected with mCherry-C1 or mCherry-TIGAR and then subjected to 1 or 6 h of OGD. (C) The marker of peroxisome, PEX14 was stained by immunocytochemistry at 6 h of reperfusion. Images shows representative examples from three independent experiments. (D) Columns represent the number of peroxisomes ($n = 30$–60 cells for each group). (E) SH-SY5Y cells were pre-transfected with 3×Flag, 3×Flag-TIGAR and then subjected to 1 or 6 h of OGD followed by 6 h of reperfusion. The Flag, TOMM20 and PEX14 level were determined by western blot ($n = 3$ from independent experiments). Numbers show the semi-quantitative analyses. Data are expressed as mean ± SEM. Statistical comparisons were performed as one-way ANOVA with Turkey's multiple-comparisons test. *$p < 0.05$, **$p < 0.01$, ***$p < 0.001$ versus the indicated group. Ctrl, control; Num., number. Mito., Mitochondrial.
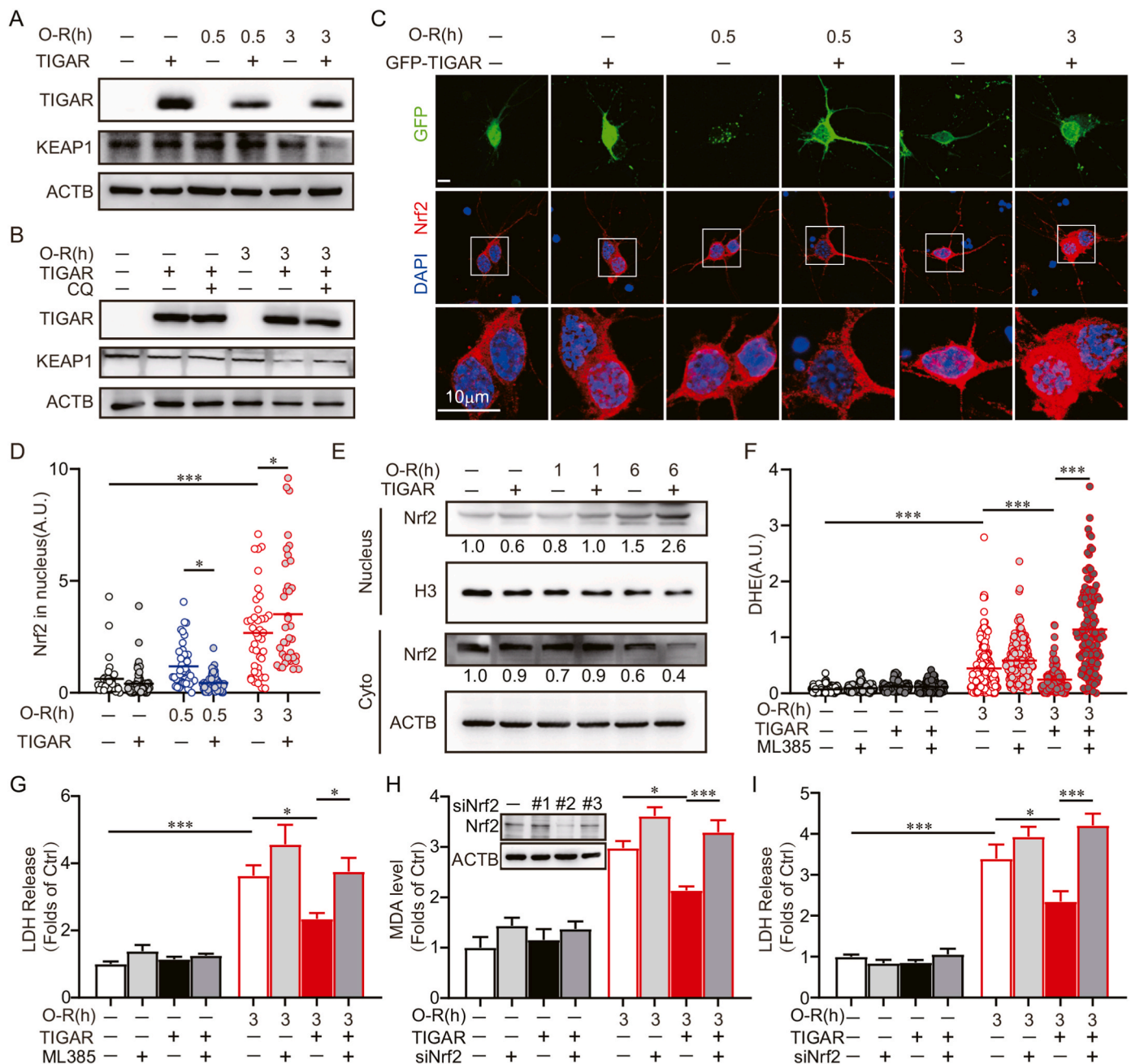
Fig. 5. TIGAR alleviates oxidative stress by activating Nrf2 in ischemic neurons. (A–D) Primary cultured cortical neurons were pre-transfected with AAVs expressing GFP -vector-3×Flag, GFP-TIGAR-3×Flag at 6 d. Experiments were conducted at 8 d. (A) Primary cultured cortical neurons were subjected to 0.5 or 3 h of OGD followed by 3 h of reperfusion. The expression of Flag and KEAP1 were determined by western blot. (B) Primary cultured cortical neurons were pretreated with 50 μM chloroquine (CQ) for 4 h before OGD and then subjected to 3 h of OGD, followed by 3 h of reperfusion. The Flag and KEAP1 levels were detected by western blot. (C) Primary cultured cortical neurons were subjected to 0.5 or 3 h of OGD and Nrf2 was stained by immunocytochemistry at 3 h of reperfusion. DAPI staining denotes the nucleus. Images shows representative examples. (D) Columns represent the fluorescence of Nrf2 in nucleus. ($n = 30$–80 cells for each group). (E)SH-SY5Y cells were pre-transfected with 3×Flag-vector or 3×Flag-TIGAR and then subjected to 1 or 6 h of OGD. The nuclear proteins were isolated from cells at 3 h of reperfusion. The Nrf2 level was determined by western blot. Numbers show the semi-quantitative analyses. (F and G) Primary cultured cortical neurons were pre-transfected with AAVs expressing GFP-vector-3×Flag, GFP-TIGAR-3×Flag at 6 d. The neurons were treated with 3 μM ML385 during OGD-Rep. Primary cultured cortical neurons were subjected to 3 h of OGD. (F) DHE fluorescence revealed ROS level at 3 h of reperfusion ($n = 120$–230 cells for each group). (G) LDH release was measured at 24 h of reperfusion. (H and I) Primary cultured cortical neurons were co-transfected with AAVs containing mCherry-3×Flag-Nrf2-shRNA and GFP-vector-3×Flag, GFP-TIGAR-3×Flag at 6 d and then subjected to 3 h of OGD at 8 d. The knockdown effect of Nrf2 was determined by western blot. #2 siNrf2 AAV was used for further experiments. (H) MDA level in neurons were determined at 3 h of reperfusion. (I) LDH release was measured at 24 h of reperfusion. All experiments are from at least three independent experiments. Data are expressed as mean ± SEM. Statistical comparisons were performed as one-way ANOVA with Turkey's multiple-comparisons test. *$p < 0.05$, **$p < 0.01$, ***$p < 0.001$ versus the indicated group. Ctrl, control; A.U., arbitrary units.
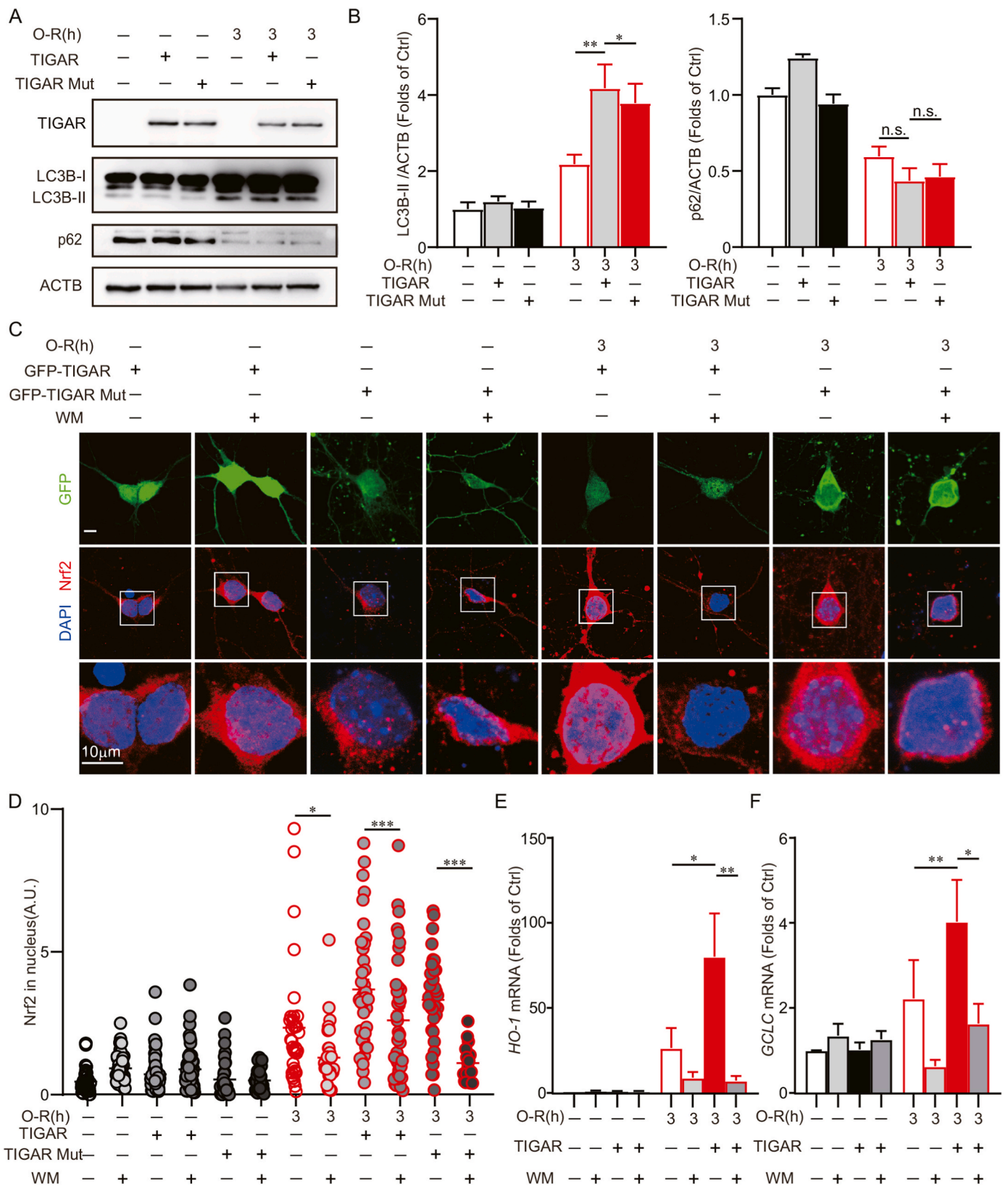
Fig. 6. Autophagy is required for TIGAR to activate Nrf2. Primary cultured cortical neurons were pre-transfected with AAVs expressing GFP-vector-3×Flag GFP-TIGAR-3×Flag or GFP-TIGAR Mutant-3×Flag at 6 d and then subjected to 3 h of OGD at 8 d. (A) The Flag, LC3B and p62 levels were determined by western blot. (B) Semi-quantitative analyses of LC3B-II and p62 are shown. (C) Wortmannin (100 nM) was administrated to neurons during OGD-Rep. Nrf2 was stained by immunocytochemistry at 3 of reperfusion. DAPI staining denotes the nucleus. Images shows representative examples. (D) Columns represent the fluorescence of Nrf2 in nucleus. ($n = 20$–80 cells for each group). The mRNA expression of (E) *HO-1* and (F) *GCLC* were measured by RT-PCR at 24 h of reperfusion. All experiments are from at least three independent experiments. Data are expressed as mean ± SEM. Statistical comparisons were performed as one-way ANOVA with Turkey's multiple-comparisons test. *$p < 0.05$, **$p < 0.01$, ***$p < 0.001$ versus the indicated group. Ctrl, control; A.U., arbitrary units.

TIGAR to activate Nrf2. We further identified the transcription of the targeted genes, *heme-oxygenase-1*(*HO-1*) and *glutamate-cysteine ligase catalytic subunit* (*GCLC*), by Nrf2. These results showed that the *HO-1* and *GCLC* genes were upregulated by TIGAR in cultured neurons with 3 h of OGD, which was reversed by wortmannin (Fig. 6E and F). All together, these data revealed that TIGAR induced autophagy and, thus, activated Nrf2 in neurons with prolonged ischemia.

3.7. TIGAR-induced autophagy alleviates oxidative stress by activating Nrf2 in mice with prolonged cerebral ischemia

We clarified whether TIGAR-conferred neuroprotection depends on autophagy and Nrf2 activation in ischemic mice brains. *Atg7*^fl/fl^ mice brains were injected with AAV-GFP-TIGAR-3×Flag and AAV-hSyn-Cre-mCherry, selectively destroying autophagy in neurons [35]. It showed that TIGAR overexpression reduced the infarct volumes and neurological deficit scores after 2 h of MCAO, which were abolished by conditional knockout of *Atg7* (Fig. 7A–C). Likewise, the knockdown of Nrf2 eliminated the neuroprotection by TIGAR in MCAO mice (Fig. 7D–F). These observations supported the idea that TIGAR-induced autophagy activated Nrf2 and protected brains against prolonged ischemia.

4. Discussion

NADPH confers the primary defense against various oxidants in ischemic brains. TIGAR is critical for NADPH generation by channeling glucose metabolism via PPP [4,5]. However, either glucose availability nor NADPH generation are impaired by prolonged duration of ischemia, regardless of the expression level of TIGAR [6,10,11]. It remains largely unclear whether and how TIGAR alleviates oxidative stress with prolonged ischemia. In the present study, we unexpectedly found that TIGAR alleviated oxidative stress in a PPP-independent manner in brains and neuronal cells with extended ischemia. In contrast, TIGAR induced autophagy, which eliminated KEAP1 and activated Nrf2, and thus neutralized this oxidative stress. Remarkably, autophagy and Nrf2 were required for TIGAR-conferred neuroprotection in ischemic mice. This previously unexplored antioxidant mechanism of TIGAR may serve as an indispensable compensation for redox homeostasis in the context of extended cerebral ischemia.

Glucose is predominantly metabolized via PPP to maintain the antioxidant status in neurons, in which Pfkfb3 is continuously degraded and, thus, diminishes F-2,6-BP production. Pfkfb3 is promptly accumulated upon oxidative stress and evokes glycolysis for bioenergetic purposes [11]. TIGAR, which is enzymatically the opposite to Pfkfb3,
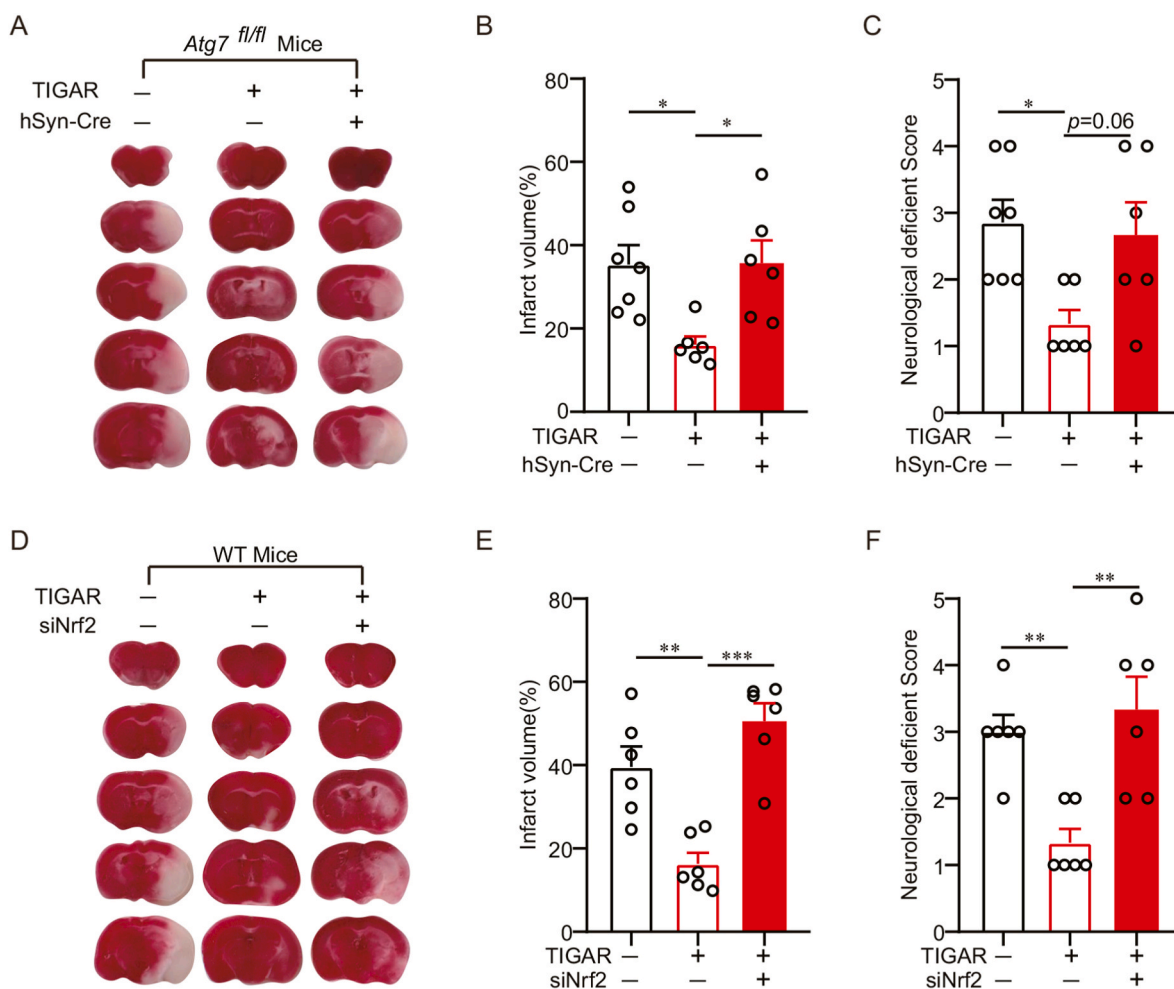
Fig. 7. TIGAR-induced autophagy alleviates oxidative stress by activating Nrf2 in mice with prolonged cerebral ischemia. (A–C) *Atg7*^fl/fl^ mice brains were co-infected with AAVs expressing hSyn-cre and GFP-vector-3×Flag or GFP-TIGAR-3×Flag for at least 3 weeks and then subjected to 2 h of MCAO. (A) The representative brain slices after TTC staining from each group are shown. (B) Infarct volumes and (C) neurological deficit scores were measured at 24 h after MCAO (n = 6–8 mice for each group). (D–F) Wild-type mice brains were co-infected with AAVs expressing Nrf2 siRNA and GFP-vector-3×Flag or GFP-TIGAR-3×Flag for at least 3 weeks and then subjected to 2 h of MCAO. (D) The representative brain slices after TTC staining are shown. (E) Infarct volumes and (F) neurological deficit scores were measured at 24 h after MCAO (n = 6–8 mice for each group). All experiments are from at least three independent experiments. Data are expressed as mean ± SEM. Statistical comparisons were performed as one-way ANOVA with Turkey's multiple-comparisons test. *$p < 0.05$, **$p < 0.01$, ***$p < 0.001$ versus the indicated group.
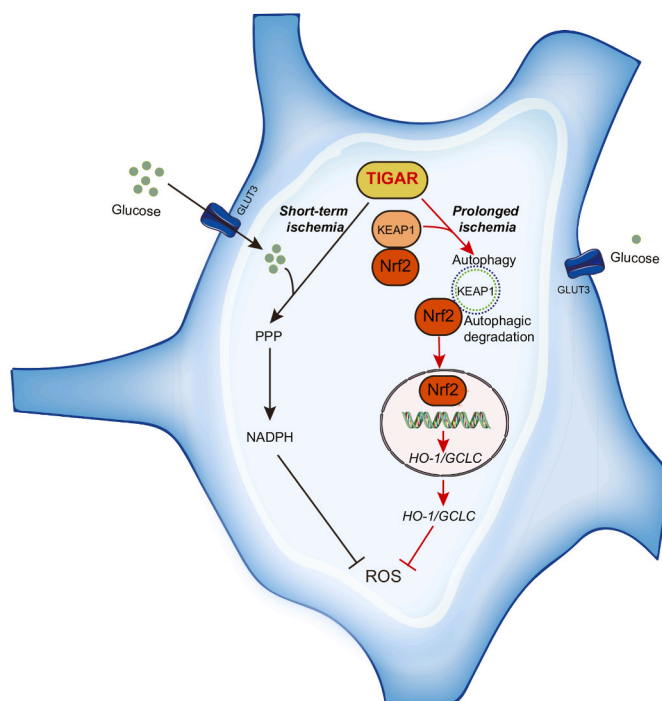
Fig. 8. The antioxidant role of TIGAR in distinct durations of cerebral ischemia. In short-term ischemia, TIGAR upregulates PPP and NADPH generation and, thus, reduces oxidative stress. With prolongation of ischemia, TIGAR induces autophagy and activates Nrf2 to neutralize oxidative stress.

alleviated oxidative stress by activating PPP in cerebral ischemia-reperfusion [6]. However, various studies have indicated that PPP is impaired in neurons with prolonged ischemia [6,11,36]. We found even TIGAR overexpression failed to reverse the decline in NADPH in either mice brains or neuronal cells that were subjected to extended ischemia (Fig. 1D and J). These observations implied that the endogenous TIGAR upregulation was insufficient to rescue oxidative stress via PPP in prolonged cerebral ischemia. Beside generating from PPP [37], NADPH can also be produced via isocitrate dehydrogenase, malic enzyme and nicotinamide nucleotide transhydrogenase [38]. However, these enzymes may have minimum effects on NADPH production during ischemia [13,39]. The incompetence of TIGAR may be attributable to the low glucose availability after prolonged ischemia [10]. Alternatively, the effects of TIGAR in ischemic neurons could be counteracted enzymatically by the accumulation of Pfkfb3, which channels glucose metabolism to glycolysis [11]. However, we surprisingly found that TIGAR can still offer antioxidative activity in prolonged ischemia (Fig. 1E and K, Fig. 5F), where NADPH has been exhausted. Moreover, neither G6PD silencing nor TIGAR mutation lacking enzymatic activity abolished the antioxidative effects of TIGAR (Fig. 1K and P). These data indicated a previously unmasked PPP-independent capacity of TIGAR in neutralizing ROS. Here, we found TIGAR overexpression promoted the translocation of Nrf2 to the nucleus and Nrf2 activation (Fig. 5C and E, Fig. 6C and D). Conversely, either pharmacological inhibition or Nrf2 silencing cancelled the antioxidant activity of TIGAR (Fig. 5F and H). Notably, it was reported that Nrf2 showed a late but sustainable activation after cerebral ischemia [28,29], which temporally coincides with TIGAR activation in prolonged ischemia. These studies indicated a distinctive route for TIGAR to counteract oxidative stress in neuronal cells. Additionally, Nrf2 induces TIGAR in cancer cells as a transcription factor [40], it cannot be excluded that Nrf2 and TIGAR may enhance each other in ischemic neurons. Taken together, TIGAR-NADPH offers transient but robust antioxidant activity, while the TIGAR-regulated Nrf2 provides a delayed but sustainable antioxidation. Given the lack of glucose after prolonged ischemia, the

PPP-independent mechanism of TIGAR provided indispensable antioxidative ability for neurons. We demonstrated the significance of Nrf2 underlying the neuroprotection by TIGAR. Either pharmacological inhibition or genetic deletion of Nrf2 cancelled the neuroprotection of TIGAR (Fig. 5G and I, Fig. 7D-F). Therefore, TIGAR-activated Nrf2 may confer essential neuroprotection to oxidative insult caused by extended ischemia injury.

Although Nrf2 controls the redox balance in ischemic brains [41], it is not fully understood how Nrf2 is triggered. Here, we provided evidence that TIGAR activated Nrf2 by the autophagic degradation of KEAP1 (Fig. 5C and E, Fig. 6C and D). The inhibition of autophagy abolished the activation of Nrf2 (Fig. 6), increased oxidative stress (Fig. 3C and D), and cancelled the neuroprotection by TIGAR (Fig. 7A–C). Moreover, the TIGAR mutation can still activate autophagy in ischemic neuronal cells (Fig. 2F and G), indicating that TIGAR-regulated Nrf2 by autophagy was independent on its PPP activity. These data emphasized that TIGAR neutralized ROS via a PPP-independent mechanism. Although previous studies indicated that TIGAR regulates autophagy [8,17–20], emerging studies have reported autophagy activation by TIGAR [21,22]. However, it remains unclear how TIGAR regulates autophagy bidirectionally. Here, we revealed the autophagy inhibition by TIGAR with short-term ischemia but autophagy activation with the prolongation of ischemia. These findings suggested the duration of ischemia may decide how TIGAR regulates autophagy. Indeed, with short-term ischemia, TIGAR acts as a switch for the PPP, promoting NADPH generation and alleviating ROS, and thus inhibiting autophagy in stroke conditions [20]. Likewise, G6PD, a rate-limiting enzyme in PPP, inhibited autophagy [42]. Conversely, Pfkfb3, an enzyme shifting PPP to glycolysis, induced autophagy [43]. These studies indicated that PPP is essential for the autophagy inhibition by TIGAR. We confirmed that TIGAR upregulated NADPH level and inhibited autophagy only after short-term ischemia. However, in neurons with prolonged ischemia, TIGAR failed to generate NADPH and activated autophagy (Fig. 1D and J). Therefore, we speculated that NADPH may alter the role of TIGAR in regulating autophagy. Our results also showed that TIGAR overexpression upregulated Beclin-1, a protein critical for autophagosome formation, suggesting TIGAR may activate autophagy (Fig. 2I). This signifies Beclin-1 may be involved in autophagy regulation by TIGAR in neurons [20]. Interestingly, TIGAR has been shown to regulate the phosphorylation of Akt, a critical signaling protein in autophagy induction [44]. This further suggests the PPP-independent mechanisms of TIGAR in the regulation of autophagy. Besides, Akt/GSK-3β phosphorylates Nrf2 and thus departs from KEAP1 after cerebral ischemia [45–47], suggesting other mechanisms for TIGAR to activate Nrf2 than KEAP1 degradation. Nevertheless, the molecular mechanisms underlying should be addressed in further studies.

5. Conclusion

Taken together, we found a PPP-independent pathway for TIGAR to alleviate oxidative stress. TIGAR induced autophagy and activated Nrf2, which offered sustainable antioxidant defense in brains with extended ischemia. This previously unexplored mechanism of TIGAR regulation may serve as a critical component of antioxidant activity caused by the lack of glucose during ischemic stroke.

Declaration of competing interest

The authors have declared that they have no conflicts of interest.

Acknowledgement

Appendix A. Supplementary data

Supplementary data to this article can be found online at https://doi.org/10.1016/j.redox.2022.102323.

References

[1] J.N. Cobley, M.L. Fiorello, D.M. Bailey, 13 reasons why the brain is susceptible to oxidative stress, Redox Biol. 15 (2018) 490–503, https://doi.org/10.1016/j.redox.2018.01.008.

[2] B. Kalyanaraman, Teaching the basics of redox biology to medical and graduate students: oxidants, antioxidants and disease mechanisms, Redox Biol. 1 (2013) 244–257, https://doi.org/10.1016/j.redox.2013.01.014.

[3] A. Herrero-Mendez, A. Almeida, E. Fernández, C. Maestre, S. Moncada, J. P. Bolaños, The bioenergetic and antioxidant status of neurons is controlled by continuous degradation of a key glycolytic enzyme by APC/C-Cdh1, Nat. Cell Biol. 11 (2009) 747–752, https://doi.org/10.1038/ncb1881.

[4] K. Bensaad, A. Tsuruta, M.A. Selak, M.N.C. Vidal, K. Nakano, R. Bartrons, E. Gottlieb, K.H. Vousden, TIGAR, a p53-inducible regulator of glycolysis and apoptosis, Cell 126 (2006) 107–120, https://doi.org/10.1016/j.cell.2006.05.036.

[5] D.R. Green, J.E. Chipuk, p53 and Metabolism: inside the TIGAR, Cell 126 (2006) 30–32, https://doi.org/10.1016/j.cell.2006.06.032.

[6] M. Li, M. Sun, L. Cao, J.H. Gu, J Ge, J. Chen, R. Han, Y.Y. Qin, Z.P. Zhou, Y. Ding, Z.H. Qin, A TIGAR-regulated metabolic pathway is critical for protection of brain ischemia, J. Neurosci. 34 (2014) 7458–7471, https://doi.org/10.1523/JNEUROSCI.4655-13.2014.

[7] M. Li, Z.P. Zhou, M. Sun, L. Cao, J. Chen, Y.Y. Qin, J.H. Gu, F. Han, R. Sheng, J. C. Wu, Y. Ding, Z.H. Qin, Reduced nicotinamide adenine dinucleotide phosphate, a pentose phosphate pathway product, might be a novel drug candidate for ischemic stroke, Stroke 47 (2016) 187–195, https://doi.org/10.1161/STROKEAHA.115.009687.

[8] Z.Q. Liu, N. Liu, S.S. Huang, M.M. Lin, S. Qin, J.C. Wu, Z.Q. Liang, Z.H. Qin, Y. Wang, NADPH protects against kainic acid-induced excitotoxicity via autophagy-lysosome pathway in rat striatum and primary cortical neurons, Toxicology 435 (2020), https://doi.org/10.1016/j.tox.2020.152408.

[9] P. Picozzi, H. Alan Crockard, R. Ross Russell, Reperfusion after Cerebral Ischemia: Influence of Duration of Ischemia, 1986. http://ahajournals.org.

[10] J. Bardutzky, Q. Shen, N. Henninger, S. Schwab, T.Q. Duong, M. Fisher, Characterizing tissue fate after transient cerebral ischemia of varying duration using quantitative diffusion and perfusion imaging, Stroke 38 (2007) 1336–1344, https://doi.org/10.1161/01.STR.0000259636.26950.3b.

[11] O. Burmistrova, A. Olias-Arjona, R. Lapresa, D. Jimenez-Blasco, T. Eremeeva, D. Shishov, S. Romanov, K. Zakurdaeva, A. Almeida, P.O. Fedichev, J.P. Bolaños, Targeting PFKFB3 alleviates cerebral ischemia-reperfusion injury in mice, Sci. Rep. 9 (2019) 1–13, https://doi.org/10.1038/s41598-019-48196-z.

[12] S. Zeng, Z. Zhao, S. Zheng, M. Wu, X. Song, Y. Li, Y. Zheng, B. Liu, L. Chen, C. Gao, H. Liu, The E3 ubiquitin ligase TRIM31 is involved in cerebral ischemic injury by promoting degradation of TIGAR, Redox Biol. 45 (2021), 102058, https://doi.org/10.1016/j.redox.2021.102058.

[13] E.T. Chouchani, V.R. Pell, E. Gaude, D. Aksentijević, S.Y. Sundier, E.L. Robb, A. Logan, S.M. Nadtochiy, E.N.J. Ord, A.C. Smith, F. Eyassu, R. Shirley, C.H. Hu, A. J. Dare, A.M. James, S. Rogatti, R.C. Hartley, S. Eaton, A.S.H. Costa, P.S. Brookes, S.M. Davidson, M.R. Duchen, K. Saeb-Parsy, M.J. Shattock, A.J. Robinson, L. M. Work, C. Frezza, T. Krieg, M.P. Murphy, Ischaemic accumulation of succinate controls reperfusion injury through mitochondrial ROS, Nature 515 (2014) 431–435, https://doi.org/10.1038/nature13909.

[14] D.H. Cho, Y.S. Kim, D.S. Jo, S.K. Choe, E.K. Jo, Pexophagy: molecular mechanisms and implications for health and diseases, Mol. Cell. 41 (2018) 55–64, https://doi.org/10.14348/molcells.2018.2245.

[15] W. Xu, U. Ocak, L. Gao, S. Tu, C.J. Lenahan, J. Zhang, A. Shao, Selective autophagy as a therapeutic target for neurological diseases, Cell. Mol. Life Sci. 78 (2021) 1369–1392, https://doi.org/10.1007/s00018-020-03667-9.

[16] R. Scherz-Shouval, Z. Elazar, Regulation of autophagy by ROS: physiology and pathology, Trends Biochem. Sci. 36 (2011) 30–38, https://doi.org/10.1016/j.tibs.2010.07.007.

[17] K. Bensaad, E.C. Cheung, K.H. Vousden, Modulation of intracellular ROS levels by TIGAR controls autophagy, EMBO J. 28 (2009) 3015–3026, https://doi.org/10.1038/emboj.2009.242.

[18] L. Ye, X. Zhao, J. Lu, G. Qian, J.C. Zheng, S. Ge, Knockdown of TIGAR by RNA interference induces apoptosis and autophagy in HepG2 hepatocellular carcinoma cells, Biochem. Biophys. Res. Commun. 437 (2013) 300–306, https://doi.org/10.1016/j.bbrc.2013.06.072.

[19] G. Tai, H. Zhang, J. Du, G. Chen, J. Huang, J. Yu, J. Cai, F. Liu, TIGAR overexpression diminishes radiosensitivity of parotid gland fibroblast cells and inhibits IR-induced cell autophagy, Int. J. Clin. Exp. Pathol. 8 (2015) 4823–4829.

[20] D.M. Zhang, T. Zhang, M.M. Wang, X.X. Wang, Y.Y. Qin, J. Wu, R. Han, R. Sheng, Y. Wang, Z. Chen, F. Han, Y. Ding, M. Li, Z.H. Qin, TIGAR alleviates ischemia/reperfusion-induced autophagy and ischemic brain injury, Free Radic. Biol. Med. 137 (2019) 13–23, https://doi.org/10.1016/j.freeradbiomed.2019.04.002.

[21] W. Zhou, Y. Yao, J. Li, D. Wu, M. Zhao, Z. Yan, A. Pang, L. Kong, TIGAR attenuates high glucose-induced neuronal apoptosis via an autophagy pathway, Front. Mol. Neurosci. 12 (2019) 1–10, https://doi.org/10.3389/fnmol.2019.00193.

[22] H. Xu, X. Xu, H. Wang, A. Qimuge, S. Liu, Y. Chen, C. Zhang, M. Hu, L. Song, LKB1/p53/TIGAR/autophagy-dependent VEGF expression contributes to PM2.5-induced pulmonary inflammatory responses, Sci. Rep. 9 (2019), https://doi.org/10.1038/s41598-019-53247-6.

[23] X. Wu, Y. Zheng, M. Liu, Y. Li, S. Ma, W. Tang, W. Yan, M. Cao, W. Zheng, L. Jiang, J. Wu, F. Han, Z. Qin, L. Fang, W. Hu, Z. Chen, X. Zhang, BNIP3L/NIX degradation leads to mitophagy deficiency in ischemic brains, Autophagy 17 (2021), https://doi.org/10.1080/15548627.2020.1802089, 1934-1946.

[24] Y. Yuan, Y. Zheng, X. Zhang, Y. Chen, X. Wu, J. Wu, Z. Shen, L. Jiang, L. Wang, W. Yang, J. Luo, Z. Qin, W. Hu, Z. Chen, BNIP3L/NIX-mediated mitophagy protects against ischemic brain injury independent of PARK2, Autophagy 13 (2017) 1754–1766, https://doi.org/10.1080/15548627.2017.1357792.

[25] D.J. Klionsky, A.K. Abdel-Aziz, S. Abdelfatah, M. Abdellatif, A. Abdoli, S. Abel, Guidelines for the use and interpretation of assays for monitoring autophagy, Autophagy 17 (2021) 1–382, https://doi.org/10.1080/15548627.2020.1797280 (4th edition)1.

[26] J.H. Zhou, T.T. Zhang, D.D. Song, Y.F. Xia, Z.H. Qin, R. Sheng, TIGAR contributes to ischemic tolerance induced by cerebral preconditioning through scavenging of reactive oxygen species and inhibition of apoptosis, Sci. Rep. 6 (2016) 1–11, https://doi.org/10.1038/srep27096.

[27] Y. Zheng, X. Zhang, X. Wu, L. Jiang, A. Ahsan, S. Ma, Z. Xiao, F. Han, Z.H. Qin, W. Hu, Z. Chen, Somatic autophagy of axonal mitochondria in ischemic neurons, JCB (J. Cell Biol.) 218 (2019) 1891–1907, https://doi.org/10.1083/JCB.201804101.

[28] N. Tanaka, Y. Ikeda, Y. Ohta, K. Deguchi, F. Tian, J. Shang, T. Matsuura, K. Abe, Expression of Keap1-Nrf2 system and antioxidative proteins in mouse brain after transient middle cerebral artery occlusion, Brain Res. 1370 (2011) 246–253, https://doi.org/10.1016/j.brainres.2010.11.010.

[29] C. Yang, X. Zhang, H. Fan, Y. Liu, Curcumin upregulates transcription factor Nrf2, HO-1 expression and protects rat brains against focal ischemia, Brain Res. 1282 (2009) 133–141, https://doi.org/10.1016/j.brainres.2009.05.009.

[30] R. Zhang, M. Xu, Y. Wang, F. Xie, G. Zhang, X. Qin, Nrf2—a promising therapeutic target for defensing against oxidative stress in stroke, Mol. Neurobiol. 54 (2017) 6006–6017, https://doi.org/10.1007/s12035-016-0111-0.

[31] R. Chen, Y.Y. Zhang, J.N. Lan, H.M. Liu, W. Li, Y. Wu, Y. Leng, L.H. Tang, J.B. Hou, Q. Sun, T. Sun, Z. Zeng, Z.Y. Xia, Q.T. Meng, Ischemic postconditioning alleviates intestinal ischemia-reperfusion injury by enhancing autophagy and suppressing oxidative stress through the Akt/GSK-3 β/Nrf2 pathway in mice, Oxid. Med. Cell. Longev. (2020), https://doi.org/10.1155/2020/6954764, 2020.

[32] S.H. Bae, S.H. Sung, S.Y. Oh, J.M. Lim, S.K. Lee, Y.N. Park, H.E. Lee, D. Kang, S. G. Rhee, Sestrins activate Nrf2 by promoting p62-dependent autophagic degradation of keap1 and prevent oxidative liver damage, Cell Metabol. 17 (2013) 73–84, https://doi.org/10.1016/j.cmet.2012.12.002.

[33] J.S. Park, D.H. Kang, D.H. Lee, S.H. Bae, Fenofibrate activates Nrf2 through p62-dependent Keap1 degradation, Biochem. Biophys. Res. Commun. 465 (2015) 542–547, https://doi.org/10.1016/j.bbrc.2015.08.056.

[34] A. Singh, S. Venkannagari, K.H. Oh, Y.Q. Zhang, J.M. Rohde, L. Liu, S. Nimmagadda, K. Sudini, K.R. Brimacombe, S. Gajghate, J. Ma, A. Wang, X. Xu, S. A. Shahane, M. Xia, J. Woo, G.A. Mensah, Z. Wang, M. Ferrer, E. Gabrielson, Z. Li, F. Rastinejad, M. Shen, M.B. Boxer, S. Biswal, Small molecule inhibitor of NRF2 selectively intervenes therapeutic resistance in KEAP1-deficient NSCLC tumors, ACS Chem. Biol. 11 (2016) 3214–3225, https://doi.org/10.1021/acschembio.6b00651.

[35] M. Komatsu, S. Waguri, T. Ueno, J. Iwata, S. Murata, I. Tanida, J. Ezaki, N. Mizushima, Y. Ohsumi, Y. Uchiyama, E. Kominami, K. Tanaka, T. Chiba, Impairment of starvation-induced and constitutive autophagy in Atg7-deficient mice, JCB (J. Cell Biol.) 169 (2005) 425–434, https://doi.org/10.1083/jcb.200412022.

[36] L. Cao, D. Zhang, J. Chen, Y.Y. Qin, R. Sheng, X. Feng, Z. Chen, Y. Ding, M. Li, Z. H. Qin, G6PD plays a neuroprotective role in brain ischemia through promoting pentose phosphate pathway, Free Radic. Biol. Med. 112 (2017) 433–444, https://doi.org/10.1016/j.freeradbiomed.2017.08.011.

[37] J.P. Bolaños, A. Almeida, The pentose-phosphate pathway in neuronal survival against nitrosative stress, IUBMB Life 62 (2010) 14–18, https://doi.org/10.1002/iub.280.

[38] F. Yin, H. Sancheti, E. Cadenas, Mitochondrial thiols in the regulation of cell death pathways, Antioxidants Redox Signal. 17 (2012) 1714–1727, https://doi.org/10.1089/ars.2012.4639.

[39] Z. Chen, Translational Medicine Research Series editors, n.d. http://www.springer.com/series/13024.

[40] H. Simon-Molas, C. Sánchez-De-Diego, À. Navarro-Sabaté, E. Castaño, F. Ventura, R. Bartrons, A. Manzano, The expression of TP53-induced glycolysis and apoptosis regulator (TIGAR) can Be controlled by the antioxidant orchestrator NRF2 in human carcinoma cells, Int. J. Mol. Sci. 23 (2022), https://doi.org/10.3390/ijms23031905.

[41] L. Liu, L.M. Locascio, S. Doré, Critical role of Nrf2 in experimental ischemic stroke, Front. Pharmacol. 10 (2019), https://doi.org/10.3389/fphar.2019.00153.

[42] L. Mele, M. la Noce, T. Paino, T. Regad, S. Wagner, D. Liccardo, G. Papaccio, A. Lombardi, M. Caraglia, V. Tirino, V. Desiderio, F. Papaccio, Glucose-6-

phosphate dehydrogenase blockade potentiates tyrosine kinase inhibitor effect on breast cancer cells through autophagy perturbation, J. Exp. Clin. Cancer Res. 38 (2019), https://doi.org/10.1186/s13046-019-1164-5.

[43] Z. Yang, J.J. Goronzy, C.M. Weyand, The glycolytic enzyme PFKFB3/phosphofructokinase regulates autophagy, Autophagy 10 (2014) 382–383, https://doi.org/10.4161/auto.27345.

[44] Z. Tang, Z. He, TIGAR promotes growth, survival and metastasis through oxidation resistance and AKT activation in glioblastoma, Oncol. Lett. 18 (2019) 2509–2517, https://doi.org/10.3892/ol.2019.10574.

[45] X. Chen, Y. Liu, J. Zhu, S. Lei, Y. Dong, L. Li, B. Jiang, L. Tan, J. Wu, S. Yu, Y. Zhao, GSK-3β downregulates Nrf2 in cultured cortical neurons and in a rat model of

cerebral ischemia-reperfusion, Sci. Rep. 6 (2016), https://doi.org/10.1038/srep20196.

[46] Autophagy Assuages Myocardial Infarction through Nrf2 Signaling Activation-Mediated Reactive Oxygen Species Clear, (n.d).

[47] R. Chen, Y.Y. Zhang, J.N. Lan, H.M. Liu, W. Li, Y. Wu, Y. Leng, L.H. Tang, J.B. Hou, Q. Sun, T. Sun, Z. Zeng, Z.Y. Xia, Q.T. Meng, Ischemic postconditioning alleviates intestinal ischemia-reperfusion injury by enhancing autophagy and suppressing oxidative stress through the Akt/GSK-3 β/Nrf2 pathway in mice, Oxid. Med. Cell. Longev. (2020), https://doi.org/10.1155/2020/6954764, 2020.